Review

Keeping Cells Alive in Microscopy

Herbert Schneckenburger * and Christoph Cremer

Posted Date: 29 November 2024

doi: 10.20944/preprints202411.2267.v1

Keywords: living cells; 3D microscopy; fluorescence; super-resolution

 doi:10.20944/preprints202411.2267.v1

Review

Keeping Cells Alive in Microscopy

Herbert Schneckenburger [1,*] and Christoph Cremer [2,3,4]

[1] Institute of Applied Research, Aalen University, 73430 Aalen, Germany
[2] Kirchhoff-Institute for Physics, University Heidelberg, 69120 Heidelberg, Germany
[3] Max Planck Institute for Polymer Research, 55128 Mainz, Germany
[4] Institute of Molecular Biology (IMB), 55128 Mainz, Germany
* Correspondence: herbert.schneckenburger@hs-aalen.de

Abstract: Light microscopy has emerged as one of the fundamental methods to analyze biological systems; novel techniques of 3D microscopy and super-resolution microscopy (SRM) with an optical resolution down to the sub-nanometer range have recently been realized. However, most of these achievements have been made with fixed specimens, i.e. direct information about the dynamics of the biosystem studied was not possible. This stimulated the development of live cell microscopy imaging approaches including Low Illumination Fluorescence Microscopy, Light Sheet Microscopy (LSM), or Structured Illumination Microscopy (SIM). Here we discuss perspectives, methods and relevant light doses of advanced fluorescence microscopy imaging to keep the cells alive at low levels of phototoxicity.

Keywords: living cells; 3D microscopy; fluorescence; super-resolution

1. Introduction

Live cell microscopy is often the basis for understanding fundamental mechanisms of cell physiology. This may be essential for detection of metabolic pathways, origin of diseases, interaction with pharmacological agents, or improved understanding of the dynamic interplay between nuclear genome structure and transcription. However, for all of these studies, cells should be kept viable and physiologically intact. This requires controlled (typically constant) temperature, availability of oxygen and nutrient fluids, cell-cell contacts, as well as low cytotoxicity and phototoxicity of molecular species involved. For optical experiments, e.g. microscopy, this implies that exposure to radiation should be minimized over a large spectrum of wavelengths. While in the ultraviolet (UV) part of the spectrum local ablation or molecular damage (e.g. DNA strand breaks, see reviews [1–3]) are dominating effects, a combination of photochemical, photothermal and opto-mechanical effects may contribute to cell damage in the visible part.

Generally, cell damage diminishes with increasing wavelength of radiation, when photon energy is no longer sufficient to induce molecular damage or ablation, and when the number of molecules absorbing light and inducing phototoxic effects decreases. This is indicated in Figure 1 showing the viability of U-373MG glioblastoma cells upon increasing light exposure with wavelengths of 375 nm, 514 nm or 633 nm. In this experiment, single cells were seeded and exposed to light doses up to 300 J/cm². Then, after 7 days the percentage of cells, which were able to form colonies (plating efficiency) was determined. Cells were regarded as viable upon less than 10% reduction of the plating efficiency at 0 J/cm², i.e. upon application of light doses up to 25, 100 or 200 J/cm² at wavelengths of 375, 514 or 633 nm, respectively. This corresponds to 4 min., 16 min. or 32 min. of solar irradiation with approximately 100 mW/cm².

Preprints.org (www.preprints.org) | NOT PEER-REVIEWED | Posted: 29 November 2024 doi:10.20944/preprints202411.2267.v1

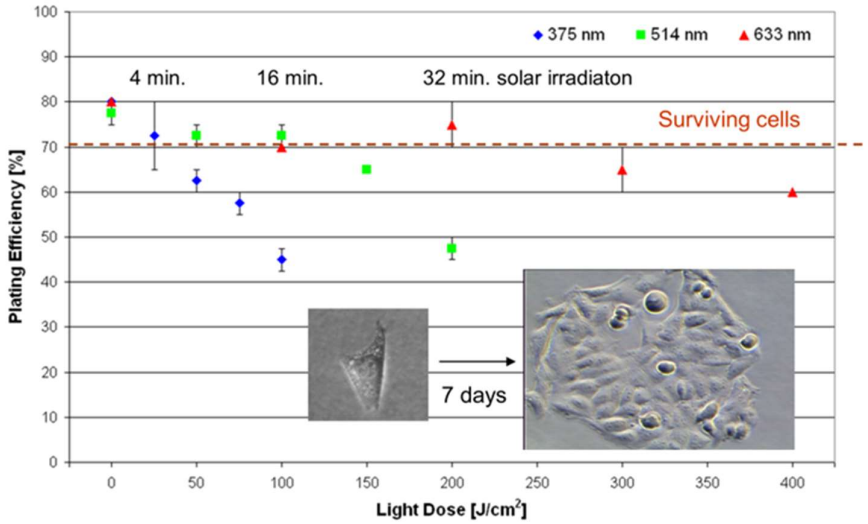

Figure 1. Plating efficiency of U373-MG glioblastoma cells upon whole cell irradiation with wavelengths of 375, 514 or 633 nm and variable light doses. Percentage of cells forming colonies within 7 days after seeding. Values represent medians ± MADs (median absolute deviations). Cells are regarded as viable upon less than 10% reduction of the plating efficiency measured at 0 J/cm², i.e. up to 25, 100 or 200 J/cm² after illumination with wavelengths of 375, 514 or 633 nm, respectively. Inset: principle of the colony-forming assay. Reproduced from [4] with modifications.

Cell viability may depend on whether irradiation occurs continuously or by short pulses and on whether whole cells or only small parts, e.g. membrane or certain organelles, are exposed to radiation. Whole cells are commonly illuminated in wide-field or laser scanning microscopy; whereas small parts are irradiated, when laser micro-beam techniques (reviewed e.g. in [5–7]) are applied. These different applications are distinguished in the Sections 2 and 3 of this manuscript.

2. Whole Cell Illumination

3.1. Mechanisms involved

- *Photochemical reactions* occur, if light is absorbed by photosensitizing molecules, which are able to transfer their excitation energy to adjacent molecules, thus creating radicals or highly reactive singlet oxygen ($^1O_2$). These species may cause photo-oxidation with subsequent cell destruction. Absorbing molecules include the coenzymes nicotinamide adenine dinucleotide (NADH, absorption maximum: 350 nm) [8] as well as flavin mono- and dinucletide (FMN/FAD; absorption maxima: 380 nm and 440 nm) [9], and porphyrin related molecules (with an absorption wavelength below 620 nm). However, while free porphyrins have a high quantum yield for creating singlet oxygen [10], this potential is reduced when porphyrins are bound within hemoglobin, myoglobin or cytochromes. At wavelengths in the far UV, the most important phototoxic effect is produced upon light absorption by DNA (with a maximum around 260 nm), which creates photo-dimers.

- *Photothermal reactions* occur upon absorption of radiation and energy conversion to heat. Main absorbers are water molecules ($\lambda \leq 250$nm, $\lambda \geq 1100$ nm), porphyrin molecules (bound e.g. within cytochromes, 350 nm $\leq \lambda \leq$ 620 nm) and proteins ($\lambda \leq 300$ nm). Thus, in the wavelength range of 620 nm $\leq \lambda \leq$ 1100 nm ("therapeutic window") absorption is comparably low, but increases at 400–600 nm, the typical excitation range for light microscopy.

- *Opto-mechanical* destruction of molecular bonds occurs at photon energies above 4 eV, corresponding to wavelengths below 300 nm. This is the spectral range of far UV or X-ray microscopy. At longer wavelengths cell or tissue disruption may occur by intensive picosecond or femtosecond laser pulses. Focusing of these laser pulses is used for ablation, hole drilling, gene

 doi:10.20944/preprints202411.2267.v1

transfection and further kinds of micro-manipulation reported in Section 3.1. However, in many applications of light microscopy these effects do not play a major role.

2.2. Microscopy methods and their compatibility with low light exposure

2.2.1. General

In Section 1, non-phototoxic light doses up to 25 J/cm² (375 nm), 100 J/cm² (514 nm) and 200 J/cm² (633 nm) were specified for native cells, i.e. cells without any staining or transfection. After staining with various blue or green absorbing dyes or transfection with a Green Fluorescent Protein (GFP) encoding plasmid, the limit of non-phototoxic light doses was often around 10 J/cm², corresponding to about 100 s of solar irradiation [4, 11]. Since this limit was about the same for continuous wave (cw) excitation and for a quasi-continuous train of short excitation pulses [11], it also holds for laser scanning or Fluorescence Lifetime Imaging (FLIM) microscopy (see below).

With a given "light dose budget" of about 10 J/cm² and a tolerable irradiance around 100 mW/cm² (solar irradiance) one can estimate a possible number of exposures under non-phototoxic conditions. Wide-field microscopy appears possible with an exposure time around one second, thus permitting about 100 images to be recorded. For Confocal ***Laser Scanning Fluorescence Microscopy (CLSM)*** [12–14] a recording time of 4–5 seconds per image is often preferable, so that 20–25 images can be measured under non-phototoxic conditions. If several layers of a sample are imaged, and if for each layer the whole sample is illuminated, this implies that a sample can be imaged with 20–25 exposures from top to bottom. For example, for a cell of 20 µm diameter, 20 selective planes shifted by 1 µm between one another in axial direction, can be recorded under physiological live cell conditions.

Figure 2 (a) shows the principal setup of CLSM with a laser beam focused to the sample. Only fluorescence signals from the focal plane (comprising its adjacent layers, as given by the optical resolution along the optical axis) can pass a small pinhole located in front of the detector (e.g. photomultiplier). By moving the sample in vertical direction, various planes can be detected (see examples in Fig. 2b,c) and combined to a 3-dimensional image. However, for recording each plane the whole sample has to be illuminated, and the light doses of each exposure sum up. An alternative technique is ***Light Sheet (Fluorescence) Microscopy***, where excitation of the sample occurs in horizontal direction, and only the illuminated plane is recorded, which is specified by the thickness of the light sheet. Therefore, the whole "light dose budget" is available for each plane, and thus this technique is preferable for long-time exposures or for repeated measurements of individual planes [15–17]. Light sheet illumination can be realized either by a cylindrical lens (usually of low or moderate aperture to reach a sufficient depth of focus) or by scanning an exciting laser beam. The light sheet depicted in Figure 2d,e) can be moved in axial direction, but for imaging individual planes the objective lens has to be shifted simultaneously. Often the shifts of the light sheet and the objective lens have to be corrected for the refractive index of the medium, where the sample is embedded. An appropriate setup for mechanical correction is described in [18], but corrections by software are also possible. Images from individual planes can be combined to a 3-D image similar to CLSM.

 doi:10.20944/preprints202411.2267.v1

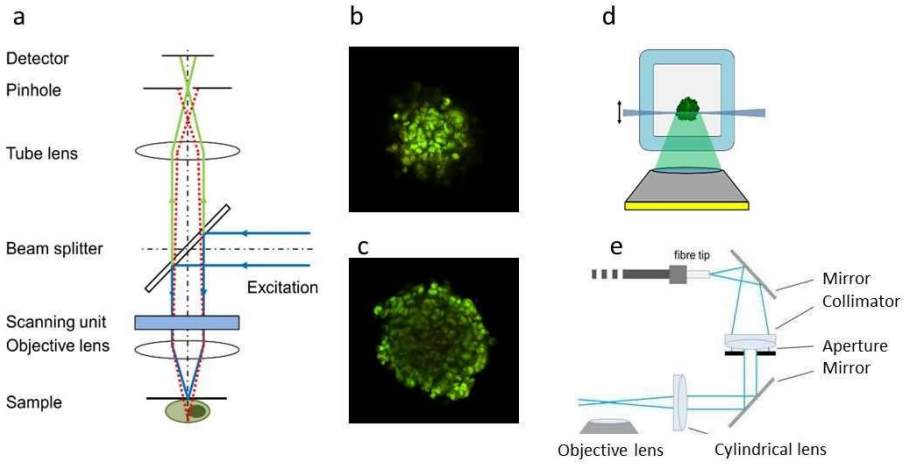

Figure 2. Principle of CLSM (a); selected planes of a cell spheroid transfected with membrane associated GFP at 15 μm (b) or 60 μm (c) from its edge (CLSM); principle (d) and technical realization of light sheet microscopy (e).

Usually the resolution in microscopy is given by the Abbe criterion $r \geq \lambda / 2\, A_N$ [19] or the Rayleigh criterion $r = 0.61\, \lambda / A_N$ [20] (with A_N corresponding to the numerical aperture of the microscope objective lens) and may attain about 200 nm for high aperture objective lenses ($A_N \geq 1.4$). Generally, the Rayleigh criterion holds for fluorescence microscopy with λ corresponding to the detection wavelength for wide-field microscopy and to the excitation wavelength for laser scanning microscopy, if the whole 0th maximum of the diffraction pattern (Airy disk) with radius 2r passes the pinhole. If the pinhole is kept smaller, the resolution can theoretically be enhanced by a factor around 1.4 [21], but the exposure time needed for each image increases, and the number of images, which can be recorded within the limiting light dose becomes much smaller. ***Airy Scan Microscopy*** (with multiple detectors behind the pinhole [21, 22]) or ***Image Scan Microscopy*** (with 2D camera detection [23]) possibly avoid this problem, since enhanced resolution may occur without diminution of fluorescence photon collection.

2.2.2. Super-resolution microscopy

During the last 30 years microscopy techniques have been developed, which substantially overcome the resolution defined by the Abbe or Rayleigh criterion. These techniques are summarized under the term ***Super-Resolution Microscopy (SRM)*** [13, 24–34] and include Airy Scan as well as Image Scan Microscopy. A further SRM method that exploits a suitable patterning of illumination to enhance resolution around a factor 2 is ***Structured Illumination Microscopy (SIM*** [35–45]). Here, the sample is commonly illuminated by two interfering laser beams (Figure 3a), typically creating a sinusoidal light pattern that may be rotated to obtain isotropic resolution in a lateral plane. Images are recorded for at least three rotation angles (e.g. 0°, 60° and 120°) and three phases (0, 2π/3, 4π/3) of the interference pattern, so that a super-resolution image is calculated from a minimum of nine individual images. Summing up the spatial frequencies k_{Abbe} resulting from the Abbe criterion and k_{IP} resulting from the interference pattern in the plane of the sample gives a resolution $r = (k_{Abbe} + k_{IP})^{-1} \geq 100$ nm (see Fig. 3b,c for a comparison with wide-field microscopy). Structured illumination appears possible at non-phototoxic conditions, but recording of 9 images for calculating one structured image implies that only about 10 SIM images can be obtained with a light dose of 10 J/cm².

 doi:10.20944/preprints202411.2267.v1

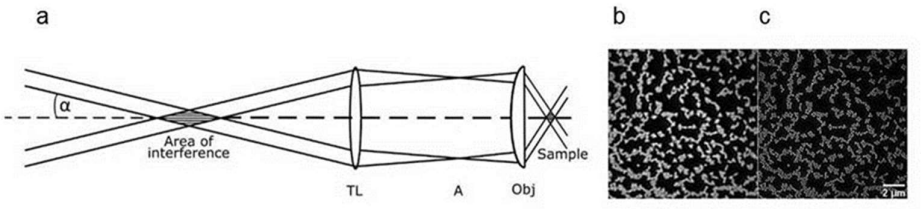

Figure 3. Principle of Structured Illumination Microscopy (SIM) with interfering first diffraction orders of an optical grating or a spatial light modulator in the focus of a collimating lens. The interference pattern is imaged in the plane of the sample by the tube lens (TL) and the microscope objective lens (Obj) with an intermediate focus in the microscope aperture A (a); Fluorescent polystyrene beads of 200 nm size recorded by wide-field microscopy (b) or SIM (c) with doubling of resolution. Reproduced from [46] with modifications.

Structured Illumination Microscopy (SIM) was used to detect mitochondria, actin filaments, as well as the Golgi apparatus dynamics in three dimensions and with high resolution [41]. Other in vivo SIM applications include 3D imaging of live neural populations [47], the dynamics of the endoplasmatic reticulum and microtubules in living cells with up to 255 frames per second [48], as well as ultra-long excitation near infrared SIM with deep tissue penetration depth of tumor microenvironments in mice [49]. The SIM principle of resolution enhancement was also used in optics with low numerical aperture A_N. The longer the wavelength, the more the light-induced generation of chemical radicals can be reduced [38]. For example, at a wavelength of 532 nm, the photochemical evaluation function according to the current safety standard [50] for 532 nm is only 1/16 of the value for 488 nm, the commonly used wavelength in commercial scanning laser opthalmology (SLO) [51]. This small phototoxicity allowed the application of structured illumination ophtalmology (532 nm) to perform super-resolving retina diagnostics of the live human eye [38]. In this case, the human eye lens with its $A_N = 0.1 – 0.3$ and a focal length ("working distance") of about 2.2 cm (ca. 130 times larger than the working distance of a typical $A_N = 1.4$ lens) was used to create on the retina a sinusoidal illumination pattern with an average intensity of about 100 mW/cm². According to safety rules [50], there was no intraocular risk even with continuous illumination at the wavelength applied. For example, a 100 s illumination would correspond to a tolerable total light dose of 10 J/cm².

In case that structured illumination is realized by interference along the optical axis using two opposite objective lenses [31, 52–54], this may enhance axial resolution with little photobleaching. In recent years, the limit of conventional axial resolution has been surpassed also by further SRM approaches including ***Standing Wave Field Microscopy (SWFM)*** [53–55], or ***Spatially Modulated Illumination (SMI) Microscopy*** [52, 56]. Experimentally, for $\lambda_{ex} = 488$ nm and an $A_N = 1.4$ objective lens, an axial resolution of about 100 nm (according to the Rayleigh criterion) has been demonstrated for SWFM, while the time integrated laser power was more than 100 times lower than required for a CLSM image of the same object [54]. Hence, for a wavelength compatible with imaging of whole live cells (e.g. 647 nm), a best optical resolution around 130 nm along the optical axis is predicted. In the case of optically isolated objects, SMI illumination has been used to determine the axial extension (size) of small, optically isolated fluorescent objects down to about 40 nm diameter with an optimal precision in the few nm range; it also allowed the axial positioning of such structures down to the 1 nm scale [52]. Since the SWFM/SMI excitation mechanisms are the same as in conventional wide-field fluorescence microscopy, these techniques allow for limitation of the irradiance and thus of the phototoxicity to the same low levels. For example, the SMI approach has been applied to measure in nuclei of live U2OS cells ($\lambda_{ex} = 488$ nm, $A_N = 1.2$ water) the size of a small chromatin domain labeled with Green Fluorescent Protein (GFP) [56].

A variety of high resolution methods are summarized under the term ***Single Molecule Localization Microscopy (SMLM)***, where individual molecules within a specimen are recorded with high precision [56–64]. If N photons are detected from a single molecule, its localization can be

 doi:10.20944/preprints202411.2267.v1

determined with a precision $\Delta x = \Delta x_0/\sqrt{N}$, with Δx_0 related to the resolution r according to the Rayleigh criterion. In the absence of background, a best precision of localization Δx = 7 nm would result from N = 100 and Δx = **3.5** nm from N = 400 [63]. Generally, however, a much higher photon budget is required [31, 57, 63].

Presently, SMLM works well for specimens up to a few μm thickness (e.g. cell monolayers), with a single molecule localization precision down to the few nm range [52, 63, 64; 87–91]; in special cases, even a sub-nm optical resolution has been realized experimentally by SMLM [57]. The thinner the sample or the illuminated part of the sample, the better are the optical conditions for imaging. In case of surface based SMLM, Total Internal Reflection Microscopy (TIRFM) [65, 66] may be applied to reduce the background, while for localization of single molecules in the interior of living cells or tissue, confocal techniques or (in individual cases) light sheet illumination [67] have been reported. Generally, SMLM techniques using homogenous wide-field illumination need an irradiance, which is typically up to several orders of magnitude larger than the irradiance in conventional microscopy, i.e. up to 50 kW/cm² [68] (see also Table 1), as well as a prolonged exposure time of a few seconds up to minutes, so that the risk of phototoxic cell damage is very high.

SMLM of fluorophores like Atto 488, GFP etc. usually requires either periodic illumination with low UV intensities and bleaching at larger wavelengths, or illumination around 488 nm, but with higher illumination intensities (kW/cm² range). Under these conditions, SMLM of unfixed cells (live at the beginning of SMLM imaging) is possible [29, 69], but a long maintenance of an undisturbed physiological state is unlikely. Since the phototoxicity decreases drastically with the wavelength used, this problem may be overcome with fluorophores, which can be excited at much longer wavelengths. For example, to image the dynamics of human histone H2B protein in living HeLa cells by SMLM at about 20 nm resolution, Wombacher et al. [70] applied ATTO655 fluorophores excited at 647 nm with an intensity of 0.5–5 kW cm^{-2}. Their data indicated that these intensities of red laser light applied for 30 min did not cause obvious single cell damage. Assuming for the HeLa cells a nuclear size of 150 μm², an illumination time of 30 min corresponded to a total dose around 1.4 J/nucleus. In other SMLM applications of live cell imaging [71], whole cell excitation intensities ≤ 10 kW/cm² at 561, 657, or 752 nm, and weak 405-nm activation intensities (typically up to 3 W/cm²), were used for membrane imaging.

To realize live cell SMLM in thick cell aggregates (50 to 150 μm, compared to a few μm for cell monolayers), Zanacchi et al. [72] used a cylindrical lens to create the required superimposed activation (405 nm) and readout (561 nm) light sheets for photactivation of monomeric Cherry (H2B-PAmCherry). Activation and readout laser intensities were 50 W cm^{-2} and 8 kW cm^{-2}, respectively; the total acquisition time was 2.5 min, with 33 frames per second, and the localization precision of single molecules was around 35 nm. With regard to the wavelengths used, the intensities applied appear to be rather high to keep the cells fully alive for a longer period. However, the possibility to study dynamic processes in live cell aggregates such as spheroids at single molecule resolution for a few minutes already should be regarded as a substantial progress. To lower the phototoxicity in live cell SMLM, the cellular area of interest might be limited, e.g. by appropriate focusing of the exciting laser beam to a cellular area of a few μm² diameter. If, for example, for a given SMLM application a whole cell irradiance of 500 W/cm² is required [70], and if instead of the whole cellular area of 200 μm², a region of interest of only 2 μm² is illuminated (e.g. containing a specifically labelled multi-protein complex, or a small chromatin domain), the total photon energy load to the cell is expected to be 100 times smaller (under else equal conditions).

Another high resolution SRM technique based on laser scanning microscopy is ***Stimulated Emission Depletion (STED) Microscopy*** [73–78]. Here, the enhancement of resolution is due to suppression of fluorescence in the outer regions of a diffraction limited illumination spot by stimulated emission using a (second) donut-shaped laser beam. While thus a resolution down to the few nm range nm has been achieved experimentally [79], the irradiance typically exceeds that of a conventional fluorescence microscope by a factor 10^4–10^5. Since fluorescence blocking by STED typically entails average intensities of a few kW/cm² over the irradiated field and several MW/cm² during the short dwell time of the laser on each spot (Airy disk), discerning fluorophores closer than

 doi:10.20944/preprints202411.2267.v1

d = 20 nm requires donut intensities of about 0.1–1 GW/cm² [80] and may cause severe damage to living specimens. Experience, however, has shown that at least for short times and small fields of view (a few μm in diameter) STED microscopy may be applied to living cells. For example, Westphal et al. [81] performed video-rate STED (28 frames per second) of fluorescently labeled synaptic vesicles with a focal spot size of 62 nanometers in live neurons, and measured the vesicles' mobility within the highly confined space of synaptic boutons. For this, the intensities applied were 3.5–6 MW/cm² for the excitation and 400 MW/cm² for the depletion beam, respectively. The average power, however, of the MaiTai Ti:Sapphire laser used (pulse width in the order of 100 fs, repetition rate 80 MHZ, tuning range in the infrared) was a few Watts only [82]. When using the photon energy, delivered e.g. by a 3 Watt laser, for a small cellular field of view of 4.5 μm² (compared to an entire cell area of about 200 μm²), one might expect that the incident photon number would be smaller by a factor (200 μm²)/(4.5 μm²). If so, STED microscopy may indeed permit live cell SRM measurements with reduced phototoxicity during short times, provided that the field of analysis is restricted to an appropriately small cellular area of interest.

Recently, the problem of high phototoxicity was reduced with the introduction of ***MINFLUX*** and ***MINSTED*** nanoscopy [80, 83–85], techniques based on the localization and tracking of single molecules in the intensity minimum of a donut-shaped laser beam. MINFLUX/MINSTED presently achieve isotropic nanometer optical resolution (presently down to about 1 nm), with a localization precision in the Angström range. In contrast to conventional STED, these methods require only moderate light exposure, since the on/off separation of spatially tight fluorophores is not performed by the doughnut, but by the on/off switching of individual fluorophores [80].

Usually only normalized intensities are provided in the literature (e.g. [83, 85]), which makes it difficult to quantitate in detail phototoxic effects. If one assumes an incident continuous wave laser beam of 1 mW being focused to an Airy disk shaped spot of 0.2 μm diameter (area 0.03 μm²), a focal intensity of about 3 MW/cm² would be estimated. This suggests that in typical CLSM imaging applications, the local irradiance during the short dwell time on a single spot may already be far above the threshold for physiological live cell imaging. If one regards the total energy dose delivered to the specimen (e.g. 60 mJ at an irradiation time of 1 min), this is relatively low. Nonetheless, 1 mW of average incident laser power distributed over an entire cellular area would still pose a non-negligible risk for undisturbed live cell observations (e.g. 500 W/cm², assuming a cellular area of 200 μm²). Table 1 summarizes the maximum light dose, typical irradiance, recording time and maximum number of images acquired under non-phototoxic conditions for various methods of light microscopy.

 doi:10.20944/preprints202411.2267.v1

Table 1. Non-phototoxic light doses and maximum number of images for various methods of 3D live cell microscopy with conventional fluorescent markers or fluorescent proteins, as deduced from Ref. 4; (*) a SIM image requires light exposure for 9 images including switching time; (**) for Single Molecule Localization Microscopy often far-read or near-infrared absorbing markers are used; for STED Microscopy red-absorbing dyes are commonly used. In both cases the maximum tolerable light doses is considerably higher than for conventional blue–green absorbing dyes. For CLSM and STED microscopy average values over the entire irradiated field (whole cells) are given. An irradiance of 100 mW/cm² corresponds approximately to solar irradiance at sea level.

Method	Max. Light Dose [J/cm²]	Irradiance [mW/cm²]	Record. Time [s]	Max. Number of Images
Wide-field microscopy	10	100	1	100
SIM	10	100	10 (*)	10
CLSM	10	100	5	20
Light Sheet (N layers)	10	100	1	N × 100
Single Molecule Localization	100 (**)	50,000 to 1,000,000	30	≤ 1
STED	10–50 (**)	3,000,000	1	≤ 1

According to Table 1 the typical illumination intensities of STED and photoswitching based SMLM [13, 31, 56–60, 62–72; 87–91] exceed by far the phototoxicity limits for longterm live cell microscopy. However, if STED/SMLM is restricted to a sufficiently short observation time, or to a small region of interest (ROI) (e.g. A_{ROI} = 1 μm² instead of 400 μm² for the total cell area A_C), the total number of photons is appropriately reduced (e.g. by the factor A_C/A_{ROI} = 400). But even this much smaller photon load appears to be still too high to keep cells viable in the sense of undisturbed proliferation capability. Nonetheless, experimental evidence [70, 83, 91] indicates that at least some specific cellular nanostructures may still be studied with these SRM methods under live cell conditions.

3. Focused Illumination

3.1. Visible irradiation

While whole cells or even larger tissue samples are illuminated in various kinds of microscopy (s. above), small areas of typically 1 μm² or less are irradiated by focused laser beams used as laser scissors, laser tweezers or optoporation systems [5–7, 92]. Mechanisms of cell damage are principally the same in both cases, however, an increasing role of multi-photon processes should be considered, when laser light is focused to small spots and often applied as ultra-short pulses. This favors local damage by opto-mechanical destruction, whereas the viability of the whole cell is less affected. Liang et al. [93] performed more detailed wavelength dependent studies of cell viability upon focused laser irradiation and found highest survival rates (percent of cells capable of clonal growth) at 800–850 nm and 950–1000 nm. Cell viability was maintained up to an irradiance of 26 MW/cm² or 52 MW/cm² and an irradiation time of 3, 5 or 10 minutes, thus corresponding to light doses between 4.68 and 31.2 GJ/cm². Schneckenburger et al. [94] specified light doses up to 1 GJ/cm² (8.3 MW/cm² within 120 s) applied around 670 nm (high power laser diode) as well as at 1064 nm (Nd:YAG laser), at which cell viability was maintained, i.e. the percentage of colony formation ("plating efficiency") was reduced by less than 10% in comparison with non-irradiated controls. At these wavelengths one-photon absorption by water and most cellular pigments as well as two-photon absorption by the coenzymes nicotinamide adenine dinucleotide (NADH) and flavin mono- or dinucleotide were rather low. This proves that non-phototoxic light doses used e.g. for laser tweezers exceed non-phototoxic light doses

 doi:10.20944/preprints202411.2267.v1

applied to whole cells by several orders of magnitude. Obviously, energy applied to a small spot may cause local damage, whereas excessive energy is dissipated over the cell and its environment, where it may reach a non-toxic level. Survival of cells in a laser tweezer system during experiments from several seconds to minutes favors numerous applications, e.g. micromanipulation [95], measurement of adhesion forces [96–98], deformability of cells [99, 100] or single cell sorting, often in combination with microfluidics or chip technologies [101, 102].

Generally, the light dose of about 10 J/cm² and the irradiance of 100 mW/cm² (solar irradiance at sea level), which are regarded as non-phototoxic for unfocused light, are increased considerably upon focusing. For example, focusing by the eye lens with a numerical aperture between 0.1 and 0.2 [103] results in an irradiance around 9 W/cm² [38] and produces almost immediately irreversible damage of the retina. Furthermore, criteria such as the proliferation rate may not sufficiently include e.g. the influence of genetic modifications on the normal physiology of the cells. On the other side, for live cell imaging directed towards analyzing on a short time level e.g. the mobility of cellular components such as transcription factors [104], or towards studying the dynamics of membrane complexes and nucleosome clusters [70, 71, 91], the maintenance of long term cellular viability will be less relevant. Hence, the acceptable photo-damage in live cell microscopy will also depend on the type of research intended.

3.2. UV irradiation

In addition to wide-field microscopy using homogeneous illumination with single-photon or multiphoton excitation [105], a variety of focused laser scanning methods has been applied for live cell imaging, such as confocal laser scanning fluorescence microscopy (CLSM), STED, Minflux/Minsted etc. (see above). The shorter (under otherwise equal conditions) the exciting wavelength, the more enhanced was the optical resolution. Hence, it should be desirable to use wavelengths as short as possible. For example, if at an excitation wavelength of 500 nm an optical lateral resolution of about 200 nm is achieved in a conventional CLSM mode, and of about 100 nm in the Airy Scan mode, the use of a wavelength of 250 nm should permit an optical resolution down to 50 nm in the Airy Scan mode. However, while such a short wavelength should be ideal from the point of view of resolution, it would produce substantial problems for live cell imaging.

For example, a UV laser microbeam with a wavelength of 257.3 nm and a minimum spot diameter of approximately 0.5 μm has been used to irradiate small regions in interphase cells of a V-79 subline of Chinese hamster cells [106]. The incident energy, which was necessary to induce a significant decrease of proliferation, was 30 to 60 times larger after micro-irradiation of the cytoplasm than after micro-irradiation of the nucleoplasm. This confirms that the most sensitive cellular target for UV irradiation is the nuclear genome. In these studies, the incident energy dose per cell, which was compatible with about 50% cell proliferation after micro-irradiation of the nucleoplasm was approximately 0.2nJ/cell nucleus, corresponding to a local energy density within the laser focus of several 10 mJ/cm². Similar energy doses applied by UV laser micro-irradiation (spot diameter about 1 μm) to live Chinese hamster interphase cells resulted in a substantial labelling of the irradiation sites by antibodies against the UV-dimers produced by the 257 nm irradiation [107]. In combination with chemical substances like caffeine, such nuclear doses were sufficient to induce severe modifications of chromatin condensation in mammalian cells [108].

To elucidate a possible effect of the distribution of UV-induced photo-lesions (pyrimidine dimers), fibroblastoid Chinese hamster cells synchronized by mitotic selection were micro-irradiated in G1 phase, using a low power UV laser microbeam (λ = 257 nm); the incident energy was either concentrated on a small part of the nucleus (mode 1) or distributed over the whole nucleus (mode 2). Following micro-irradiation the cells were incubated with 3H-thymidine for 2 h and thereafter processed for autoradiography. The findings [109] suggested that within the investigated range of energy doses (≈ 0.4 nJ/nucleus to 150 nJ/nucleus) and local energy densities (≈ 0.3 mJ/cm² to 100 mJ/cm²), the total amount of unscheduled DNA synthesis (UDS) depends on the total number of dimers, but not on their spatial distribution in nuclear DNA.

 doi:10.20944/preprints202411.2267.v1

Low doses of laser UV microirradiation (257 nm) were reported to induce also severe effects on embryonic development in insects [110]. Here, Drosophila embryos were locally irradiated with a 257 nm laser UV microbeam during blastoderm and germ band stages. The doses used did not eliminate nuclei or cells at once, but up to 50% of the adult survivors from irradiated eggs carried defects in the thorax. In these studies, a laser spot of 10 µm diameter (energy: 500 or 1,000 nJ) resulted in a local energy density of 160 mJ/cm² and a local illumination intensity of 635 mW/cm² , or 1,270 mW/cm²; a laser spot of 20 µm diameter corresponded to a local light exposure of 160 mW/cm² or 320 mW/cm², respectively. Irradiation of wild-type Drosophila blastoderms with a UV laser microbeam of 20 µm focal spot diameter and local energy densities of about 200 mJ/cm² (total energy doses about 700 mJ/nucleus) frequently resulted in localized cuticle defects in the ensuing larvae [111].

The low thresholds for cellular phototoxicity after UV micro-irradiation, with a wavelength (257 nm) in the absorption maximum of DNA, may be compared with the effects produced at longer wavelengths with homogeneous illumination. Due to their functional role, retina cells appear to be specially suited to explore the physiological limits of phototoxicity. For example, in studies with apes, Höh et al. [112] – using a wavelength of 441 nm and 1000 s of illumination of the Fovea with an energy density of 30 J/cm² (corresponding to an intensity of 30 mW/cm² during the exposure time of 1,000s) – did not induce a visus reduction. 60 J/cm² (60 mW/cm²) resulted in a temporary visus reduction after 5 days and a recovery after 20-30 days; at 90 J/cm² (90 mW/cm²) a permanent visus reduction without recovery was observed. Assuming an average area of retina cell nuclei of 150 µm², (30–90 J/cm²), this would correspond to an energy dose in the range of (4.5–13.5) x 10^{-5} J/nucleus, i.e. around 4 orders of magnitude higher than at 257 nm (see above). To conclude, available experimental evidence confirms the statements that typically live cell fluorescence microscopy imaging using wavelengths above 530 nm and illumination intensities below 100 mW/cm² for whole cell irradiation, can be performed with physiologically intact cells.

4. Discussion and Conclusion

For many years, light microscopy of fixed specimens has been one of the most important research tools of biology and medicine. Microscopy of live cells was restricted to relatively few special cases; although its possibility had already been demonstrated by Antony van Leeuwenhoek when he first observed live structures later known as bacteria [113]. For many reasons, it became more and more desirable to apply microscopy also to live cells. The invention of phase microscopy [114] was a first most important step – presently used in all biomedical laboratories worldwide to monitor e.g. cell cultures – and a necessary tool for a variety of cell manipulations such as cloning [115, 116]. However, such imaging approaches do not readily allow for the detailed analysis of specific cellular structures. Therefore, appropriate discrimination is required, using e.g. fluorescence techniques. While in fixed cells this enabled an extended light microscopic image analysis of most specific cell components, down to individual proteins, RNA and DNA sequences, even at nanometer resolution, it created substantial challenges to keep the cells simultaneously alive. In this report, a short overview is given on the state of the art of microscopy imaging with respect to its use in live cell analysis, such as wide field microscopy, Confocal Laser Scanning Microscopy (CLSM) or Light Sheet Fluorescence Microscopy (LSFM), as well as Super Resolution Microscopy (SRM) including Structured Illumination Microscopy (SIM), Stimulated Emission depletion (STED) microscopy with its variants (MINFLUX/MINSTED) and Single Molecule Localization Microscopy (SMLM). To obtain a criterion for the applicability of such imaging methods in view of keeping cells alive, we considered in particular the photonic burden (illumination intensity, total energy delivered) in connection with these methods. Some main conclusions are:

-The most sensitive cellular target with respect to cellular viability (in terms of proliferation potential) is the cell nucleus;

-In whole cell irradiation, a profound dependence on the illuminating wavelength exists: while far UV light (absorption maximum of nucleic acids) is highly damaging, the phototoxicity decreases considerably with increasing excitation wavelength;

-Super-Resolution Fluorescence Microscopy with linear excitation modes (e.g. SIM, MINFLUX, linear excitation localization) and wavelengths with low photonic energy is largely compatible with a live cell status, especially if restricted to a small cellular region of interest;

-Live cell applications of Super-Resolution Fluorescence microscopy using non-linear excitation modes (e.g. photoswitching based SMLM; STED) appear to be possible under specific conditions (such as long excitation wavelengths, small fields of illumination), in particular for short-term analyses of cellular nanostructures.

Software-based solutions may further contribute to reduce the phototoxicity towards living cells. In 2008 Hoebe et al. reported on a method called Controlled Light Exposure Microscopy (CLEM) with a non-uniform illumination of the field of view [117]. This permits to reduce the light exposure in strongly fluorescent parts of the sample and thus the total number of excited fluorophore molecules. Possibly self-learning algorithms will help in the future to control the illumination of each pixel exactly such that its fluorescence can be well detected and localized and that its phototoxicity can be kept at a minimum. Further development in camera and sensor technology as well as photo-stable fluorescent dyes and novel labeling procedures (using e.g. nanographenes, [118]) will contribute to an optimization of fluorescence imaging with low phototoxicity even down to the single-molecule level.

Author Contributions: H.S. and C.C. wrote this manuscript and contributed equally to the text.

Funding: This review received no external funding

Institutional Review Board Statement: Not applicable

Informed Consent Statement: Not applicable.

Data Availability Statement: Not applicable.

Acknowledgment: This manuscript includes the authors' own experiments in cooperation with David Baddeley, Gerrit Best, Udo Birk, Sarah Bruns, Thomas Bruns, Thomas Cremer, Michael Hausmann, Rainer Heintzmann, Margit Lohs-Schardin, Verena Richter, Florian Schock, Michael Wagner, Petra Weber, and Christian Zorn.

Conflicts of Interest: The authors declare no conflict of interest.

References

1. Cadet, J.; Berger, M.; Douki, T.; Morin, B.; Raoul, S.; Ravanat, J.L.; Spinelli, S. Effects of UV and visible radiation on DNA-final base damage. *Biol. Chem.* **1997**, *378(11)*, 1275–1286.
2. Nakanishi, M.; Niida, H.; Murakami, H.; Shimada, M. DNA damage responses in skin biology – implications in tumor prevention and aging acceleration. *J. Dermatol. Sci.* **2009**, *56(2)*, 76–81. https://doi.org/10.1016/j.jdermsci.2009.09.001.
3. Richa; Sinha, R.P.; Häder, D.P. Physiological aspects of UV-excitation of DNA. *Top. Curr. Chem.* **2015**, *356*, 203–248. https://doi.org/10.1007/128_2014_531.
4. Schneckenburger, H.; Richter, V.; Wagner, M. Live-cell optical microscopy with limited light doses. SPIE Spotlight Series, Vol. SL 42, **2018**, 38 pages, ISBN: 9781510622593.
5. Berns, M.W. A history of laser scissors (microbeams). *Methods Cell Biol.* **2007**, *82*, 1–58. https://doi.org/10.1016/S0091-679X(06)82001-7.
6. Ashkin, A. Optical trapping and manipulation of neutral particles using lasers. *Proc. Natl. Acad. Sci. USA* **1997**, *94*, 4853–4860. https://doi.org/10.1073/pnas.94.10.4853.
7. Greulich, K.O. *Micromanipulation by light in biology and medicine: the laser microbeam and optical tweezers*. Birkhäuser, Basel-Boston-Berlin, 1999.
8. Scott, T.G.; Spencer, R.G.; Leonard, N.J.; Weber, G. Emission properties of NADH. Studies of fluorescence lifetimes and quantum efficiencies of NADH, AcPyADH and simplified synthetic models. *J. Am. Chem. Soc.* **1970**, *92*, 687–695.
9. Galland, P.; Senger, H. The role of flavins as photoreceptors. *J. Photochem. Photobiol. B* **1988**, *1*, 277–294.
10. Ormond, A.B.; Freeman, H.S. Dye Sensitizers for Photodynamic Therapy. *Materials (Basel)* **2013**, *6(3)*, 817–840. https://doi.org/10.3390/ma6030817.
11. Schneckenburger, H.; Weber, P.; Wagner, M.; Schickinger, S.; Richter, V.; Bruns, T.; Strauss, W.S.; Wittig, R. Light exposure and cell viability in fluorescence microscopy. *J. Microsc.* **2012**, *245(3)*, 311–318. https://doi.org/10.1111/j.1365-2818.2011.03576.x.
12. Jonkman, J.; Brown, C.M.; Wright, G.D.; Anderson, K.I.; North, A.J. Tutorial: guidance for quantitative confocal microscopy. *Nat. Protoc.* **2020**, *1585–1611*. https://doi.org/10.1038/s41596-020-0313-9.
13. Ehrenberg M. The Nobel Prize in Chemistry **2014** (Press Release). http://www.nobelprize.org/nobel_prizes/chemistry/laureates/2014/advanced-chemistryprize2014.pdf.

14. Masters, B.R. **1996**. Selected Papers on Confocal Microscopy, SPIE Milestone Series, volume MS 131, SPIE Optical Engineering Press, Bellingham.
15. Huisken, J.; Swoger, J.; del Bene, F.; Wittbrodt, J.; Stelzer, E.H.K. Optical sectioning deep inside live embryos by SPIM. *Science* **2004**, *305(5686)*, 1007–1009. https://doi.org/10.1126/science.1100035.
16. Santi, P.A. Light sheet fluorescence microscopy: a review. *J. Histochem. Cytochem.* **2011**, *59(2)*, 129–138. https://doi.org/10.1369/0022155410394857.
17. Pampaloni, F.; Chang, B.-J.; Stelzer, E.H.K. Light sheet-based fluorescence microscopy (LSFM) for the quantitative imaging of cells and tissues. *Cell Tissue Res.* **2015**, *360(1)*, 129–141. https://doi.org/10.1007/s00441-015-2144-5.
18. Bruns, T.; Schickinger, S.; Schneckenburger, H. Single plane illumination module and micro-capillary approach for a wide-field microscope. *J. Vis. Exp.* **2014**, *15(90)*, e51993. https://doi.org/10.3791/51993.
19. Abbe, E. Beiträge zur Theorie des Mikroskops und der mikroskopischen Wahrnehmung. Arch. Mikrosk. Anat. 1873, 9, 413–418. https://doi.org/10.1007/BF02956173.
20. Rayleigh, L. On the Theory of Optical Images, with Special Reference to the microscope. 1896. The London, Edinburgh, and Dublin Philosophical Magazine and Journal of Science 42, Part XV, 1896, pp. 167–195.
21. Wu, X.; Hammer, J.A. ZEISS Airyscan: Optimizing Usage for Fast, Gentle, Super-Resolution Imaging. *Methods Mol. Biol.* **2021**, *2304*, 111–130. https://doi.org/10.1007/978-1-0716-1402-0_5.
22. Weisshart, K. The Basic Principle of Airyscanning. Carl Zeiss, 2014. https://pages.zeiss.com/rs/896-XMS-794/images/ZEISS-Microscopy.
23. Müller, C.B.; Enderlein, J. Image Scanning Microscopy. *Phys. Rev. Lett.* **2010**, *104*, 198101. https://doi.org/10.1103/physrevlett.104.198101.
24. Cremer, C.; Masters, B.R. Resolution enhancement techniques in microscopy. *Eur. Phys. J. H* **2013**, *38*, 281–344. https://link.springer.com/article/10.1140/epjh/e2012-20060-1.
25. Sydor, A.M. ; Czymmek, K.J.; Puchner, E.M. ; Mennella, V. Super-resolution microscopy: from single molecules to supramolecular assemblies. *Trends Cell Biol.* **2015**, *25*, 730–748. https://doi.org/10.1016/j.tcb.2015.10.004.
26. Galbraith C.G.; Galbraith, J.A. Super-resolution microscopy at a glance. *J Cell Sci*. **2011**, *124*, 1607–1611. https://doi.org/10.1242/jcs.080085.
27. Toraldo di Francia, G. Resolving power and information. *J. Opt. Soc. Am.* **1955**, *45*, 497–499. https://doi.org/10.1364/JOSA.45.000497.
28. Cox, S. Super-resolution imaging in live cells. *Dev. Biol.* **2015**, *40*, 175–181. https://doi.org/10.1016/j.ydbio.2014.11.025.
29. Cremer, C.; Kaufmann, R.; Gunkel, M.; Pres S.; Weiland, Y.; Müller, P. et al. Superresolution imaging of biological nanostructures by spectral precision distance microscopy. *Biotechnol. J.* **2011**, *6*, 1037–1051. https://doi.org/10.1002/biot.201100031.
30. Shtengel, G.; Galbraith, J.A.; Galbraith, C.G.; J. Lippincott-Schwartz, J.; Gillette, J.M.; ManleyS. et al. Interferometric fluorescent super-resolution microscopy resolves 3D cellular ultrastructure. *Proc. Natl. Acad. Sci. USA* **2009**, *106*: 3125–3130. https://doi.org/10.1073pnas.0813131106.
31. Birk, U. Super-Resolution Microscopy-A Practical Guide. Wiley-VCH, Weinheim/Germany, 2017. ISBN: 978-3-527-34133-7.
32. Heintzmann, R. Answers to fundamental questions in superresolution microscopy. *Phil. Trans. R.Soc. A* **2021**, *379*: 20210105. https://doi.org/10.1098/rsta.2021.0105.
33. Schermelleh, L.; Ferrand, A.; Huser, T.; Eggeling, C.; Sauer, M.; Biehlmaier, O.; Drummen, G. P. C. Super-resolution microscopy demystified. *Nature Cell Biology* **2019**, 21, 72–84. https://doi.org/10.1038/s41556-018-0251-8.
34. Fornasiero, E. F.; Opazo, F. Super-resolution imaging for cell biologists: Concepts, applications, current challenges and developments. *Bioessays* **2015**, *37*, 436–451. https://doi.org/10.1002/bies.201400170.
35. Gustafsson, M.G.; Shao, L.; Carlton, P.M.; Wang, C.J.R.; Golubovskaya, I.N.; Cande, W.Z.; Agard, D.A.; Sedat, J.W. Three-Dimensional Resolution Doubling in Wide-Field Fluorescence Microscopy by Structured Illumination. *Biophys. J.* **2008**, *94*, 4957–4970. https://doi.org/10.1529/biophysj.107.120345.
36. Hirvonen, L.M.; Wicker, K.; Mandula, O.; Heintzmann, R. Structured illumination microscopy of a living cell. *Eur. Biophys. J.* **2009**, *38*, 807–812. https://doi.org/10.1007/s00249-009-0501-6.
37. Heintzmann, R., Cremer, C. Lateral modulated excitation microscopy: Improvement of resolution by using a diffraction grating. *Proc. SPIE* **1999**, 3568, 185–196. https://doi.org/10.1117/12.336833.
38. Schock, F.; Best, G.; Celik, N.; Heintzmann, R.; Dithmar, S.; Cremer, C. Structured illumination ophthalmoscope: super-resolution microscopy on the living human eye. *Phil. Trans. R. Soc. A* **2022**, *380*, 20210151. https://doi.org/10.1098/rsta.2021.0151
39. Allen, J.R.; Ross, S.T.; Davidson, M.W. Structured illumination microscopy for superresolution. *Chem. Phys. Chem.*. **2014**, *15*, 566–576. https://doi.org/10.1002/cphc.201301086.40.

40. Chakrova, N., Heintzmann, R., Rieger, B., Stallinga, S. Studying different illumination patterns for resolution improvement influorescence microscopy. *Opt Exp.* **2015**, *23*, 31367–31383. https://doi.org/10.1364/oe.23.031367.
41. Li, D.; Shao, L.; Chen, B.-C.; Zhang, X.; Zhang, M.; Moses, B. et al. Extended resolution structured illumination imaging of endocytic and cytoskeletal dynamics. *Science* **2015**, *349*, aab3500. https://doi.org/10.1126/science.aab3500.
42. Gustafsson, M.G.L. Nonlinear structured-illumination microscopy: wide-field fluorescence imaging with theoretically unlimited resolution. *Proc Natl Acad. Sci. USA* **2005**, 102,13081–13086, https://doi.org/10.1073/pnas.0406877102.
43. Heintzmann, R.; Huser, T. Super-resolution structured illumination microscopy. *Chem. Rev.* **2017**, *117*, 13890–13908. https.//doi.org/10.1021/acs.chemrev.7b00218.
44. Gustafsson, M. G. L. Surpassing the lateral resolution limit by a factor of two using structured illumination microscopy. *J. Microsc*. **2000,** *198*, 82–87. https://doi.org/10.1046/j.1365-2818.2000.00710.x.
45. Kraus, F.; Miron, E.; 2, Demmerle, J.; Chitiashvili, T.; Budco, A.; Alle, Q. et al. Quantitative 3D structured illumination microscopy of nuclear structures. *Nature Protocols* **2017**, *12(5)*, 1011 – 1027. https://doi.org/10.1038/nprot.2017.020.
46. Schneckenburger, H. Lasers in Live Cell Microscopy. *Int. J. Mol. Sci.* **2022**, 23, 5015. https://doi.org/10.3390/ijms23095015.
47. Supekar, O.D.; Sias, A.; Hansen, S.R.; MartinezG.; Peet, G.C.; Peng, X. et al. Miniature structured illumination microscope for in vivo 3D imaging of brain structures with optical sectioning. *Biomed. Opt. Exp.* **2022**, *13(4)*, 2531. https://doi.org/10.1364/BOE.449533.
48. Löschberger, A.; Novikau, Y.; Netz, R.; Kleppe, I.; Spindler, M.-C.; Benavente, R.; et al. Super-Resolution Imaging by dual iterative structured illumination microscopy, Carl Zeiss, **2017**. https://www.zeiss.com/microscopy/en/products/light-microscopes/super-resolution-microscopes/elyra-7.html?
49. Wang, F.; Ma, Z.; Zhong, Y.; Salazar, F.; Xu, C.; Ren F.; et al. In vivo NIR-II structured-illumination light-sheet microscopy. *Proc Natl Acad. Sci. USA* **2021**, 118, No. 6, e2023888118. https://doi.org/10.1073/pnas.202388811.
50. ISO 15004-2:2007: Ophthalmic instruments — Fundamental requirements and test methods, Part 2: Light hazard protection. International Organization for Standardization 2019. https://www.iso.org/standard/38952.html.
51. Fischer, J.; Otto, T.; Delori, F.; Pace, L.; Staurenghi, G. Scanning Laser Ophthalmoscopy (SLO). In: High Resolution Imaging in Microscopy and Ophthalmology. New Frontiers in Biomedical Optics (Bille JF, editor), Springer **2019**. https://www.ncbi.nlm.nih.gov/books/NBK554043/.
52. Cremer, C.; Schock, F.; Failla, A.V.; Birk, U. Modulated illumination microscopy: Application perspectives in nuclear nanostructure analysis. *J. Microsc.* ***2024***, 1–8. https://doi.org/10.1111/jmi.13297.
53. Lanni, F.; Bailey, B.; Farkas, D.L.; Taylor, D.L. Excitation field synthesis as a means for obtaining enhanced axial resolution in fluorescence microscopes. *Bioimaging* **1993**, *1*, 187–196. http://dx.doi.org/10.1002/1361-6374(199312)1:4%3C187::AID-BIO1%3E3.0.CO;2-P.
54. Frohn, J.; Knapp, H.; Stemmer, A. True optical resolution beyond the Rayleigh limit achieved by standing wave illumination. *Proc. Natl. Acad. Sci. USA* **2000**, *97*, 7232–7236.
55. Bailey; B., Farkas, D.; Taylor, D.L.; Lanni, F. Enhancement of axial resolution in fluorescence microscopy by standing-wave excitation. *Nature* **1993**, *366*, 44–48. https://www.nature.com/articles/366044a0.
56. Reymann, J.; Baddeley, D.; Gunkel, M.; Lemmer, P.; Stadter, W.; Jegou, T. et al. High precision structural analysis of subnuclear complexes in fixed and live cells via spatially modulated illumination (SMI) microscopy. *Chromosome Res.* **2008**, *16*, 367–382. https://doi.org/10.1007/s10577-008-1238-2.
57. Reinhardt, S.C.M.; Masullo, L.A.; Baudrexel, I.; Stehen, Ph.R.; Kowalewski, K.; Eklund, A.S. et al. Ångström-resolution fluorescence microscopy. *Nature* **2023**, *617*, 711–716. https://doi.org/10.1038/s41586-023-05925-9.
58. Betzig, E.; Patterson, G.H.; Sougrat, R.; Lindwasser, O.W.; Olenych, S.; Bonifacino, J.S.; Davidson, M.W.; Lippincott-Schwartz, J.; Hess, H.F. Imaging intracellular fluorescent proteins at nanometer resolution. *Science* **2006**, *313*, 1642–1645. https://doi.org/10.1126/science.1127344.
59. Rust, M.J.; Bates, M.; Zhuang, X. Sub-diffraction-limit imaging by stochastic optical reconstruction microscopy (STORM). *Nat. Methods* **2006**, *3*, 793–796. https://doi.org/10.1038/nmeth929.
60. Hess, S.T.; Girirajan, T.P.; Mason, M.D. Ultra-High Resolution Imaging by Fluorescence Photoactivation Localization Microscopy. *Biophys. J.* **2006**, *91*, 4258–4272. https://doi.org/10.1529/biophysj.106.091116.
61. Cox, S.; Rosten, E.; Monypenny, J.; Jovanovic-Talisman, T.; Burnette, D.T.; Lippincott-Schwartz, J.; E Jones, G.; Heintzmann, R. Bayesian localization microscopy reveals nanoscale podosome dynamics. *Nat. Methods* **2011**, *9*, 195–200. https://doi.org/10.1038/nmeth.1812.
62. Ha, T. Single-molecule methods leap ahead. *Nature Methods* **2014**, *11*, 1015–1018. https://doi.org/10.1038/nmeth.3107.

63. Cremer, C.; Szczurek, A.; Schock, F.; Gourram, A.; Birk, U. Super-resolution microscopy approaches to nuclear nanostructure imaging. *Methods* **2017**, *123*, 11–32. https://doi.org/10.1016/j.ymeth.2017.03.019.
64. Gelléri, M.; Chen, S.-Y.; Hübner, B.; Neumann, J.; Kröger, O.; Sadlo, F. et al. True-to-scale DNA-density maps correlate with major accessibility differences between active and inactive chromatin. *Cell Reports* **2023**, *42*, 112567. https://doi.org/10.1016/j.celrep.2023.112567.
65. Reck-Peterson, S.L.; Derr, N.D.; Stuurman, N. Imaging single molecules using total internal reflection fluorescence microscopy (TIRFM). Cold Spring Harb. Protoc. 2010, pdb.top73. https://doi.org/10.1101/pdb.top73.
66. Luo, W.; He, K.; Xia, T.; Fang, X. Single-molecule monitoring in living cells by use of fluorescence microscopy. *Anal. Bioanal. Chem*. **2013**, *405(1)*, 43–49. https://doi.prg/10.1007/s00216-012-6373-0.
67. Ritter, J.G.; Veith, R.; Veenendaal, A.; Siebrasse, J.P.; Kubitscheck, U. Light Sheet Microscopy for Single Molecule Tracking in Living Tissue. *PLoS ONE* **2010**, *5*, e11639. https://doi.org/10.1371/journal.pone.0011639.
68. Barentine, A.E.S.; Lin, Y.; Courvan; E.M.; Kidd. Ph.; Liu, M.; Balduf, L. et al. An integrated platform for high-throughput nanoscopy. *Nature Biotechnology* **2023**, *41*, 1549–1556. https://www.nature.com/articles/s41587-023-01702-1.
69. Lakadamyali, M. Super-Resolution Microscopy: Going Live and Going Fast. *Chem. Phys. Chem.* **2014**, *15*, 630–636. https://doi.org/10.1002/cphc.201300720.
70. Wombacher, R.; Heidbreder, M.; van de Linde, S.; Sheetz, M.P.; Heilemann, M.; Cornish, V.W.; Sauer, M. Live-cell super-resolution imaging with trimethoprim conjugates. *Nature Methods* **2010**, *7*, 717–719. https://doi.org/10.1038/nmeth.1489.
71. Shim, S.-H.; Xi, C.; Zhonga,G.; Babcocka, H.P.; Vaughana, J.C.; Huanga, B.; Wang, X. et al. Super-resolution fluorescence imaging of organelles in live cells with photoswitchable membrane probes. *Proc. Natl. Acad. Sci. USA* **2012**, *109*, 13978–13983. https://doi.org/10.1073/pnas.1201882109.
72. Zanacchi, F.C.; Lavagnino, Z.; Donnorso, M. P.; Del Bue, A.; Furia, L.; Faretta, M.; Diaspro, A. Live-cell 3D superresolution imaging in thick biological samples. *Nature Methods* **2017**, *8(12*), 1047–1049.
73. Hell, S.W.; Wichmann, J. Breaking the diffraction resolution limit by stimulated emission: stimulated-emission-depletion fluorescence microscopy. *Opt. Lett.* **1994,** *19(11)*, 780–782. https://doi.org/10.1364/ol.19.000780.
74. Wildanger, D.; Medda, R.; Kastrup, L.; Hell, S. A compact STED microscope providing 3D nanoscale resolution. *J. Microsc.* **2009**, *236*, 35–43. https://doi.org/10.1111/j.1365-2818.2009.03188.x.
75. Blom, H.; Widengren, J. STED microscopy—towards broadened use and scope of applications. *Curr. Opin. Chem. Biol.* ***2014***, *20*, 127–33. https://doi.org/10.1016/j.cbpa.2014.06.004.
76. Hofmann, M.; Eggeling, C.; Jakobs, S.; Hell, S.W. Breaking the diffraction barrier in fluorescence microscopy at low light intensities by using reversibly photoswitchable proteins. *Proc. Natl. Acad. Sci. USA* 2005, *102*, 17565–17569. https://doi.org/10.1073/pnas.0506010102.
77. Hell, S.W. 2009. Microscopy and its focal switch. Nature Methods 2009, 6, 24–32. https.//doi.org/10.1038/nmeth.1291.
78. Chmyrov, A.; Keller, J.; Grotjohann, T.; Ratz, M.; d'Este, E., Jakobs, S. et al. Nanoscopy with more than 100,000 'Doughnuts.' *Nature Methods* **2013**, *10*, 737–40. https://doi.org/10.1038/nmeth.2556.
79. Rittweger, E., Han, K.Y.; Irvine, S.E.; Eggeling, C.; Hell. S.W. STED microscopy reveals crystal colour centres with nanometric resolution. *Nature Photonics* **2009**, *3*, 144147.
80. Weber, M.; Leutenegger, M.; Stoldt, S.; Jakobs, S.; Mihaila, T.S.; Butkevich, A.N.; Hell, S.W. MINSTED fluorescence localization and nanoscopy. *Nature Photonics* **2021**, *15*, 361–366. https://doi.org/10.1038/s41566-021-00774-2.
81. Westphal, V.; Rizzoli, S.O.; Lauterbach, M.A.; Kamin, D.; Jahn, R.; Hell, S.W.Video-Rate far-field optical nanoscopy dissects synaptic vesicle movement. *Science* **2008**, *320*, 246–249. doi/epdf/10.1126/science.1154228.
82. Mai Tai® One Box Ti:Sapphire Ultrafast Lasers. Spectra Physic,. 2014. https://www.spectra-physics.com/en/f/mai-tai-ultrafast-laser.
83. Balzarotti, F.; Eilers, Y.; Gwosch, K.C.; Gynnå, A.H.; Westphal, V.; Stefani, F.D.; Elf, J.; Hell, S.W. Nanometer resolution imaging and tracking of fluorescent molecules with minimal photon fluxes. *Science* **2016**, *355*, 606–612. https://doi.org/10.1126/science.aak9913.
84. Gwosch, K. C.; Pape, C.; Balzarotti, J.K.; Hoess, F.; Ellenberg, P.; Ries, J.; Hell, S. W. MINFLUX nanoscopy delivers 3D multicolor nanometer resolution in cells. *Nature Methods* **2020**, *17*,217–224.
85. Sahl, S. J.; Matthias, J.; Inamdar, K.; Weber, M.; Khan, T. A.; Brüser, C.; Jakobs, S.; Becker, S.; Griesinger, C.; Broichhagen, J.; Hell, S.W. Direct optical measuerement of intramolecular distances with Angström precision. *Science* **2024**, *386*, 180–187. https://doi.org/10.1126/science.adj7368.
86. Jonkman, J.; Brown, C.M.; Wright, G.D.; Anderson, K.I.; North, A.J. Tutorial: guidance for quantitative confocal microscopy. *Nature Protocols* **2020**, 1585–1611. https://www.nature.com/nprot.

87. Huang, B.; Wang, W.; Bates, M.; Zhuang, X. Three-dimensional super-resolution imaging by stochastic optical reconstruction microscopy. *Science* **2008**, *319*, 810–3. https://doi.org/10.1126/science.1153529.
88. Heilemann, M.; van de Linde, S.; Schüttpelz, M.; Kasper, R.; Seefeldt, B.; Mukherjee, A. et al. Subdiffraction-resolution fluorescence imaging with conventional fluorescent probes. *Angew. Chem. Int. Ed.* **2008**, *47*, 6172–6176. https://doi.org/10.1002/anie.200802376.
89. Lemmer, P.; Gunkel, M.; Baddeley, D. et al. SPDM: light microscopy with single-molecule resolution at the nanoscale. *Appl. Phys. B* **2008**, 93, 1–12. https://doi.org/10.1007/s00340-008-3152-xP.
90. Huang, B.; Jones, S.A.; Brandenburg, B.; Zhuang, X. Whole-cell 3D STORM reveals interactions between cellular structures with nanometer-scale resolution. *Nature Methods* **2008**, *5*, 1047–1052. https://doi.org/10.1038/nmeth.1274.
91. Ricci, M.A.; Manzo, C.; Garcıa-Parajo, M.F.; Lakadamyali, M.; Cosma, M.P. Chromatin fibers are formed by heterogeneous groups of nucleosomes in vivo. *Cell* **2015**, *160*, 1145–1158. https://doi.org/10.1016/j.cell.2015.01.054.
92. Schneckenburger H. Laser-assisted optoporation of cells and tissues – a mini-review. *Biomed. Opt Express* **2019**, *10(6)*, 2883–2888. https://doi.org/10.1364/BOE.10.002883.
93. Liang, H.; Vu, K.T.; Krishnan, P.; Trang, T.C.; Shin, D; Kimel, S.; Berns, M.W. Wavelength dependence of cell cloning efficiency after optical trapping. *Biophys. J.* **1996**, *70(3)*, 1529–1533. https://doi.org/10.1016/S0006-3495(96)79716-3.
94. Schneckenburger, H.; Hendinger, A.; Sailer, R.; Gschwend, M.H.; Strauss, W.S.; Bauer, M.; Schütze, K. Cell viability in optical tweezers: high power red laser diode versus Nd:YAG laser. *J. Biomed. Opt.* **2000**, *5(1)*, 40–44. https://doi.org/10.1117/1.429966.
95. Greulich, K.O. Manipulation of cells with laser microbeam scissors and optical tweezers: a review. *Rep. Prog. Phys*. **2017**, *80(2)*, 026601. https://doi.org/10.1088/1361-6633/80/2/026601.
96. Khalili, A.A.; Ahmad, A.R. A Review of Cell Adhesion Studies for Biomedical and Biological Applications. *Int. J. Mol. Sci.* **2015**, *16(8)*, 18149–18184. https://doi.org/10.3390/ijms160818149.
97. Park, S.; Kim, J.; Yoon, S.H. A Review on Quantitative Measurement of Cell Adhesion Strength, *J. Nanosci. Nanotechnol.* **2016**, *16(5)*, 4256–4273.
98. Arbore, C.; Perego, L.; Sergides, M.; Capitanio, M. Probing force in living cells with optical tweezers: from single-molecule mechanics to cell mechanotransduction. *Biophys. Rev.* **2019**, 765–782. https://doi.org/10.1007/s12551-019-00599-y.
99. Musielak, M. Red blood cell-deformability measurement: review of techniques, *Clin. Hemorheol. Microcirc.* **2009**, *42(1)*, 47–64. https://doi.org/10.3233/CH-2009-1187.
100. Priezzhev, A.; Lee, K. Potentialities of laser trapping and manipulation of blood cells in hemorheologic research. *Clin. Hemorheol. Microcirc.* **2016**, *64(4)*, 587–592 (2016). https://doi.org/10.3233/CH-168030. PMID: 27767983.
101. Arai, F.; Ng, C.; Maruyama, H.; Ichikawa, A.; El-Shimy, H.; Fukuda, T. On chip single-cell separation and immobilization using optical tweezers and thermo-sensitive hydrogel. *Lab Chip* **2005**, *5(12)*, 1399–1403. https://doi.org/10.1039/b502546j.
102. X. Wang, X.; Chen, S.; Kong, M.; Wang, Z.; Costa, K.D.; Li, R.A.; Sun, D. Enhanced cell sorting and manipulation with combined optical tweezer and microfluidic chip technologies. *Lab Chip* **2011**, *11(21)*, 3656–3662. https://doi.org/10.1039/c1lc20653b.
103. Kaschke, M.; Donnerhacke, K.-H.; Rill, M.S. Optical Devices in Ophthalmology and Optometry: Technology, Design Principles, and Clinical Applications, **2014**, Wiley. https://doi.org/10.1002/9783527648962.
104. Szczurek, A.T.; Dimitrova, E.; Kelley, J.R. et al. The Polycomb system sustains promoters in a deep OFF state by limiting pre-initiation complex formation to counteract transcription. *Nature Cell Biol.* 2024, **26**, 1700–1711. https://doi.org/10.1038/s41556-024-01493.
105. Peker, B.; Rausch, M. Microscopy of Organoids. Breakthrough in live cell microscopy of 3D cellular models. *Microscopy and Analysis* **2020**, *34(2)*, 15–17.
106. Cremer, C.; Cremer, T.; Zorn, C.; Schoeller, L. Effects of laser-uv-microirradiation (λ = 257 nm) on proliferation of Chinese hamster cells. *Radiat. Res*. **1976**, *66*, 106–121. PMID: 1257404.
107. Cremer, C.; Cremer, T.; Fukuda, M.; Nakanishi, K. Detection of Laser-uv-microirradiation induced DNA photolesions by immunofluorescent staining. *Hum. Genet.* **1980**, *54*, 107–110. https://link.springer.com/article/10.1007/BF00279058.
108. Zorn, C.; Cremer, T.; Cremer, C.; Zimmer, J. Laser-uv-micro-irradiation of interphase nuclei and posttreatment with caffeine: A new approach to establish the arrangement of interphase chromosomes. *Hum. Genet.* **1976**, *35*, 83–89. https://link.springer.com/article/10.1007/BF00295622.
109. Cremer, C.; Cremer, T.; Jabbur, G. Laser-uv-microirradiation of Chinese hamster cells: The influence of the distribution of photolesions on unscheduled DNA synthesis. *Photochem. Photobiol.* **1981**, *33*, 925–928. https://doi.org/10.5282/ubm/epub.9311.

110. Lohs-Schardin, M.; Sander ,K.; Cremer, C.; Cremer, T.; Zorn, C. Localized ultraviolet laser microbeam irradiation of early Drosophila embryos: Fate maps based on location and frequency of adult defects. *Develop. Biol.* **1979**, *68*, 533–545. https://doi.org/10.1016/0012-1606(79)90224-0.
111. Nüsslein-Volhard, Ch.; M. Lohs-Schardin, M.; K. Sander, K.; C. Cremer, C. A dorso-ventral shift of embryonic primordia in a new maternal-effect mutant of Drosophila. *Nature* **1980**, *283*, 474 - 476. https://doi.org/10.1038/283474a0.
112. Höh, A.E.; Ach, T.; Amberger, R.; Dithmar, S. Lichtexposition bei vitreoretinaler Chirurgie. *Ophthalmologe* **2008**. https://doi.org/10.1007/s00347-008-1794-z.
113. https://en.wikipedia.org/wiki/Antonie_van_Leeuwenhoek.
114. Zernike, F. Das Phasenkontrastverfahren bei der mikroskopischen Beobachtung. *Phys. Zeitschr.* **1935**, *36*, 848–851.
115. Campbell, K.; McWhir, J.; Ritchie, W. et al. Sheep cloned by nuclear transfer from a cultured cell line. *Nature* **1996**, *380*, 64–66. https://doi.org/10.1038/380064a0.
116. Wilmut, I;, Schnieke, A.; McWhir, J. et al. Viable offspring derived from fetal and adult mammalian cells. *Nature* **1997**, *385*, 810–813. https://doi.org/10.1038/385810a0.
117. Hoebe, R.A.; Van der Voort, H.T.; Stap, J.; Van Noorden, C.J.; Manders, E.M. Quantitative determination of the reduction of phototoxicity and photobleaching by controlled light exposure microscopy. *J Microsc.* **2008**, *231(Pt 1)*, 9–20. https://doi.org/10.1111/j.1365-2818.2008.02009.x
118. Zhu, X.; Chen, Q.; Zhao, H. et al. Intrinsic Burst-Blinking Nanographenes for Super-Resolution Bioimaging. *J. Am. Chem. Soc.* **2024**, *146*, 5195−5203. https://doi.org/10.1021/jacs.3c11152.